

# VideoAssembler: Identity-Consistent Video Generation with Reference Entities using Diffusion Model

Haoyu Zhao<sup>1</sup> Tianyi Lu<sup>1</sup> Jiaxi Gu<sup>2</sup> Xing Zhang<sup>1</sup>

Zuxuan Wu<sup>1</sup> Hang Xu<sup>2</sup> Yu-Gang Jiang<sup>1</sup>

<sup>1</sup> Fudan University, China <sup>2</sup> Huawei Noah's Ark Lab, China

<sup>1</sup>{hyzhao22@m., luty22@m., zhangxing18@, zxwu@, ygj@}fudan.edu.cn

<sup>2</sup>{imjiaxi, chromexbjxh}@gmail.com



Figure 1. We propose VideoAssembler, a novel method for generating videos with diverse contents, guided by the reference entities (left) and text prompts (below). It can preserve the fidelity of the entity and generate controllable content.

## Abstract

Identity-consistent video generation seeks to synthesize videos that are guided by both textual prompts and reference images of entities. Current approaches typically utilize cross-attention layers to integrate the appearance of the entity, which predominantly captures semantic attributes, resulting in compromised fidelity of entities. Moreover, these methods necessitate iterative fine-tuning for each new entity encountered, thereby limiting their applicability. To address these challenges, we introduce VideoAssembler, a novel

end-to-end framework for identity-consistent video generation that can conduct inference directly when encountering new entities. VideoAssembler is adept at producing videos that are not only flexible with respect to the input reference entities but also responsive to textual conditions. Additionally, by modulating the quantity of input images for the entity, VideoAssembler enables the execution of tasks ranging from image-to-video generation to sophisticated video editing. VideoAssembler comprises two principal components: the Reference Entity Pyramid (REP) encoder and the Entity-Prompt Attention Fusion (EPAF) module. The

*REP encoder is designed to infuse comprehensive appearance details into the denoising stages of the stable diffusion model. Concurrently, the EPAF module is utilized to integrate text-aligned features effectively. Furthermore, to mitigate the challenge of scarce data, we present a methodology for the preprocessing of training data. Our evaluation of the VideoAssembler framework on the UCF-101, MSR-VTT, and DAVIS datasets indicates that it achieves good performances in both quantitative and qualitative analyses (346.84 in FVD and 48.01 in IS on UCF-101). Our project page is at <https://gulu captain.github.io/videoassembler/>.*

## 1. Introduction

Video generation [8, 11, 13, 37, 42] is recently a hot topic and a vital research challenge. This technology holds great promise for various applications, such as marketing, advertising, and social media content creation. Text-to-video [5, 8, 9, 11, 37] is a common approach for video generation that guides the semantic content of the generated video with the text condition but cannot control its detailed structure. Therefore, some works [5, 18, 25, 27, 43] explore image-to-video synthesis, where the image condition provides more visual information for the generation. However, these methods fail to preserve the detailed visual appearance of input entities, resulting in a generation of diminished fidelity. This research direction has significant advantages, and the task of synthesizing topic-specific videos from given images has various potential applications.

Identity-consistent video generation is a challenging task, as it requires not only generating content-reasonable videos but also injecting the given entity information into videos reasonably. Existing methods [4, 25] attempt to incorporate the subject identity into the generated videos by adding new temporal and spatial information to the cross-attention layers. The identity consistency of their generated videos is not satisfactory, as they suffer from appearance fidelity and weak action guidance. Besides, they are based on a few-shot fine-tuning paradigm, which means they require retraining the model for each new entity during inference. Hence, existing methods are inadequate to address identity-consistent video generation tasks effectively.

To alleviate these problems, we propose a novel method, referred to as “VideoAssembler”, that aims at preserving the identity of reference entities while generating videos of high quality. We show some of our generated videos in Fig. 1, and we can find that our method achieves high entity fidelity and the input entity can be flexibly generated and precisely controlled by prompts. Moreover, similar to [25], by taking the entities from a video as the input data, our model can also be flexibly adapted to a video editing framework that can perform subject-preserving video editing tasks. Our VideoAssembler is an end-to-end method, which can do inference directly on different entities. It con-

tains two parts, i.e., the Reference Entity Pyramid (REP) encoder and the Entity-Prompt Attention Fusion (EPAF) module. The REP encoder is designed as a hierarchical structure to encode multi-scale entity images, which can improve the representation ability of the encoder and adapt to entities of different sizes. Compared with existing methods [23, 43, 47], which directly use the UNet downsampling structure or CLIP model to encode the image condition, our REP encoder has good reconstruction effects and can effectively introduce detailed appearance into the denoising steps. The EPAF module is employed to introduce the image embeddings to the cross-attention layer of UNet. This operation can bring text-alignment information to the model, which is helpful in generating highly relevant videos. Besides, due to the lack of data, we design a data-process approach to prepare the training data. Our model undergoes validation through a multifaceted experimental framework, encompassing the assessment of video generation metrics on UCF-101 [38] and MSR-VTT [45], along with video editing metrics on the DAVIS [14] dataset. The outcomes indicate that VideoAssembler attains good performance in both quantitative and qualitative evaluations.

In short, our work makes the following contributions:

- We propose VideoAssembler, an end-to-end framework designed for identity-consistent video generation, demonstrating the capability to conduct direct inference when giving new entities without additional training. Moreover, through the control of quantities per entity, it can enable image-to-video generation and video editing tasks.
- Comprising two novel components, REP and EPAF, VideoAssembler exhibits noteworthy effects in generating videos characterized by adaptability to input entities and responsiveness to textual conditions.
- Experimental results on UCF-101, MSR-VTT, and DAVIS datasets show that our method achieves good results in both quantitative and qualitative evaluations. We get results of 346.84 in FVD and 48.01 in IS on UCF-101.

## 2. Related Work

### 2.1. Text-guided Video Generation

Diffusion models(DMs) [17] shows astonishing ability in image generation [16, 19, 26, 29, 32, 33]. Motivated by image generation via DMs, several works explore DMs for video generation. Video diffusion model (VDM) [12] is introduced by modifying 2D U-Net in image diffusion models to 3D U-Net. Existing video generation methods use textual prompts to control the video generation, such as [1, 8–11, 13]. These methods mainly add temporal layers to a pre-trained latent diffusion model and fine-tune the temporal layers. Among these methods, PYoCo [8] and VidRD [9] stand out within the realm of video synthesis, demonstrating notable achievements in the generation domain.

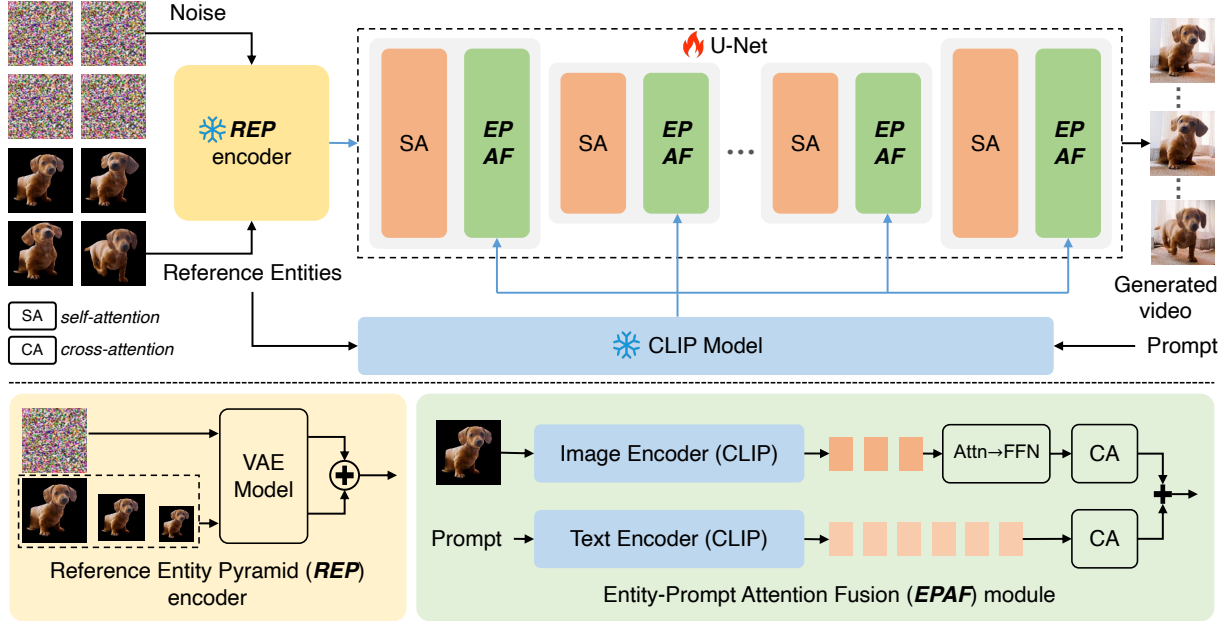


Figure 2. The training pipeline of our VideoAssembler method. The model can generate high-fidelity videos according to the given entities and text prompts. We train all the attention layers encompassed within the U-Net, while maintaining the VAE and CLIP models frozen.

## 2.2. Image-guided Video Generation

Except for the textual control, many methods [21, 27] try to employ images as the condition of video generation. For example, the first frame is generally selected as the image condition. The key to image-to-video is adding motion features to the objects in the image. VideoComposer [43] combines the spatial condition (image) and temporal conditions (depth and video) to control the video synthesis. VideoCrafter1 [5] takes both the text and image prompts as the inputs and feeds them into the spatial transformer via cross-attention. I2VGen-XL [48] contains two major stages to get high-resolution videos. The model is trained on large-scale video and image data and then fine-tuned on small high-quality data. In addition, existing works also employ human pose [18, 24, 31, 41], human motion [6, 46], and sound [15] to control the content.

## 2.3. Identity-consistent Video Generation

Although considerable progress has been made in the field of text-to-video and image-to-video domains, identity-consistent generation is still a challenging task, especially in video generation, and the new domain has received increasing attention. In the image synthesis domain, the Subject-Diffusion [23] model proposes a novel open-domain personalized image generation model. It can generate identity-consistent images with multiple subjects provided by users without fine-tuning. In the video generation domain, Dreamix [25] proposes a fine-tuning method to finish identity-consistent video generation, which creates

videos based on image and text inputs. VideoDreamer [4] focuses on generating videos with multiple subjects. The model customizes its generator by using the Disen-Mix finetuning strategy to tackle the attribute binding problem.

Existing methods that aim for identity consistency often fall short in maintaining the attributes of visual entities. The multifaceted nature and diversity of real-world entity content present significant challenges to these approaches. Additionally, these methods typically introduce entity features directly into the cross-attention layer, which predominantly provides a coarse-grained visual representation. Furthermore, the dependency of these methods on the fine-tuning paradigm necessitates retraining for novel subjects, thereby constraining their applications.

## 3. Method

Generating a video of a certain entity, given a sequence of static appearances of it, is nontrivial. Both temporal consistency and fidelity are challenging. For this purpose, we propose VideoAssembler, and the training pipeline is shown in Fig. 2. VideoAssembler is designed to generate videos of high fidelity and quality, which are conditioned by reference entity and text prompt. Unlike existing fine-tuning methods [4, 25, 34], VideoAssembler is an end-to-end framework capable of performing direct inference with a diverse array of entities. The quantity of input entity images can be flexibly determined, with even a single image being adequate as the minimum requirement. Our method is based on VidRD [9], which is a pure text-to-video model, includ-

ing a VAE for latent representation and U-Net for latent denoising. VideoAssembler contains two parts, i.e., Reference Entity Pyramid (REP) encoder and Entity-Prompt Attention Fusion (EPAF) module. Besides, due to the limitation of training data, we also contribute to a new data process approach. We introduce the overview of VideoAssembler and the preliminaries in Sec. 3.1, REP in Sec. 3.2, EPAF in Sec. 3.3, and data process in Sec. 3.4.

### 3.1. Overview and Preliminaries

Video processing consumes more computation than image processing because video consists of multiple frames. Compared to calculating directly on pixel space, most existing synthesis methods [8, 11, 25] work on latent space. We also choose to generate videos from latent space. LDMs aim to learn the underlying data distribution by applying iterative denoising steps to samples from a noise distribution.

VideoAssembler accepts two inputs: the reference entity and the textual prompt. The textual prompt is directly utilized as input to the CLIP model to obtain textual tokens, while the reference entity undergoes processing through the REP and EPAF components, respectively. On one hand, the encoding of noise and input entities is accomplished through the utilization of the REP encoder. This process is reversible via the VAE decoder. Subsequently, the concatenation of video latent  $\mathbf{z}_0^v$  and entity latent  $\mathbf{z}_0^e$  representations is employed, and the concatenated feature  $\mathbf{z}_0$  is subsequently inputted into a U-Net architecture. In the diffusion forward process, Gaussian noise is added to  $\mathbf{z}_0$  iteratively, denoted as Eq. (1), where  $t = 1, 2, \dots, T$ .

$$q(\mathbf{z}_t | \mathbf{z}_{t-1}) = \mathcal{N}(\mathbf{z}_t; \sqrt{1 - \beta_t} \mathbf{z}_{t-1}, \beta_t \mathbf{I}) \quad (1)$$

where  $T$  is the number of diffusion timesteps and  $\beta_t$  is the noise level at timestep  $t$ . In the backward process, the latent  $\mathbf{z}_0$  is recovered from  $\mathbf{z}_T$  step by step via U-Net. In our framework, the U-Net architecture is characterized by the integration of two distinct types of temporal layers: *Temp-conv*, denoting three-dimensional convolution layers, and *Temp-Attn*, signifying temporal attention layers. On the other hand, the entity is introduced into the CLIP model alongside a projection layer. In the EPAF module, the entity feature and prompt feature are then fused after cross-attention. Subsequently, the latent representation undergoes an iterative denoising process, progressively refining its quality. Finally, the ultimate generated video is decoded utilizing the VAE decoder.

### 3.2. Reference Entity Pyramid Encoder

Text-to-video synthesis methods utilize textual prompts to direct the content generation within the resulting video. However, prompts primarily concentrate on the semantic-level specifications, rather than providing granular control over the detailed appearance [5]. Consequently, the strong

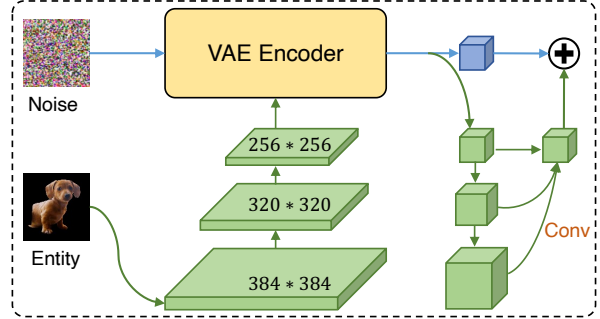


Figure 3. The structure of our REP encoder, which is architecturally hierarchical and accepts inputs at three distinct resolutions. This design ensures the preservation of the entity’s integrity, enabling the synthesis of high-fidelity representations of the entity.

influence of prompt leads to a level of input entity control that is unpredictable and may not align with the outcome.

To maintain the high fidelity of the input entity, we propose a REP encoder for VideoAssembler, shown in Fig. 3. The architecture of this encoder is designed as a pyramid structure, wherein the VAE model is utilized to introduce the detailed appearance into U-Net. The hierarchical architecture of the REP enables the learning of features across multiple scales and granularities, encapsulating both local and global characteristics of the entity. Additionally, this structure is apt for processing smaller entities and enhances the robustness of the model against variations in orientation and instances of partial occlusion. Given video data  $\mathbf{x}_0^v$  and the entity data  $\mathbf{x}_0^e$ , the  $\mathbf{x}_0^e$  is sampled into three kinds of sizes,  $384 \times 384$ ,  $320 \times 320$  and  $256 \times 256$  are chosen empirically. The video and the sampled entity undergo processing by the VAE model.

Many previous approaches [23, 43] leverage the capabilities of the CLIP model to extract image features. However, a salient limitation of CLIP lies in the non-generative nature of its vision encoder. It is capable solely of mapping visual data into a reduced-dimensional vector space, yet it lacks the functionality to reconstruct or generate images in a reverse process. Compared with CLIP, VAE confers a distinct advantage through its capacity to explicitly model the distribution of latent variables. This attribute is not only exceptionally conducive to the encoding of video data but also when employed as an entity encoder, it can enhance the preservation of specific information throughout the denoising process. We also conduct experiments of our method w/o REP encoder in the ablation studies.

Therefore, we choose the VAE model to encode the three kinds of  $\mathbf{x}_0^e$ . The video data is projected into video latent  $\mathbf{z}_0^v$  and the entity is projected into entity latent  $\mathbf{z}_0^e$ . Similar to the process of input video in Eq. (1), Gaussian noise is

added to entity  $\mathbf{z}_0^e$  iteratively, denoted as Eq. (2).

$$q(\mathbf{z}_t^e | \mathbf{z}_{t-1}^e) = \mathcal{N}(\mathbf{z}_t^e; \sqrt{1 - \beta_t} \mathbf{z}_{t-1}^e, \beta_t \mathbf{I}) \quad (2)$$

Due to the disparate output dimensions of VAE processing, specifically those with dimensions of  $384 \times 384$  and  $320 \times 320$ , the employment of two distinct convolutional layer architectures (*conv.s*) is necessitated to maintain uniformity in feature dimensionality. Finally, the total latent is represented as Eq. (3), where  $\oplus$  is a concatenate operation.

$$\mathbf{z}_0 = \mathbf{z}_0^v \oplus \mathbf{z}_0^e \quad (3)$$

The latent  $\mathbf{z}_0$  is fed into U-Net for denoising.

### 3.3. Entity-Prompt Attention Fusion

We introduce the entity into U-Net through the REP encoder. Nevertheless, the misalignment between the feature representations derived from the VAE and prompt features processed by the CLIP model engenders a limitation within the model. Although the REP encoder exhibits a proficient capability for entity feature integration, this misalignment reduces the granular ability of text-driven detail generation within the resultant video synthesis. To improve the details of the generated videos, we employ the CLIP features like image models [5, 23, 43]. These models demonstrate that visual tokens possess a control capability analogous to that of textual prompts. For this purpose, we employ the EPAF module, as Fig. 2 shows (bottom-right). This module mainly brings textual alignment entity features into cross attention, which treats the entity feature as a text-like condition to obtain the global entity feature.

Given the entity image  $\mathbf{x}_0^e$  and text prompt, the prompt is encoded with CLIP in Stable Diffusion [33] model, and the entity image is handled using the CLIP model which is trained on LAION-2B data [36]. We use all the visual tokens from the last layer to represent the image feature. The image tokens are then handled with an attention layer and several linear layers, which are denoted as  $\text{Proj}(\text{Attn}(\text{CLIP}(\mathbf{x}_0^e)))$ . Then, the two features are put into the cross-attention layers of U-Net. We share the value of  $q$  and train the  $k_1, v_1$  values of prompt and  $k_2, v_2$  values of entity, respectively. This process is represented as Eq. (4).

$$\mathbf{F} = \text{Softmax}\left(\frac{\mathbf{Q}\mathbf{K}_1^\top}{\sqrt{d}}\right)\mathbf{V}_1 + \text{Softmax}\left(\frac{\mathbf{Q}\mathbf{K}_2^\top}{\sqrt{d}}\right)\mathbf{V}_2 \quad (4)$$

### 3.4. Training Data Process

The VideoAssembler is an end-to-end method that needs training on the video dataset, which encompasses paired text-video data along with their corresponding segmentation masks. Due to the lack of existing suitable training data, we propose an automated data processing methodology that segments the entity within a video to construct

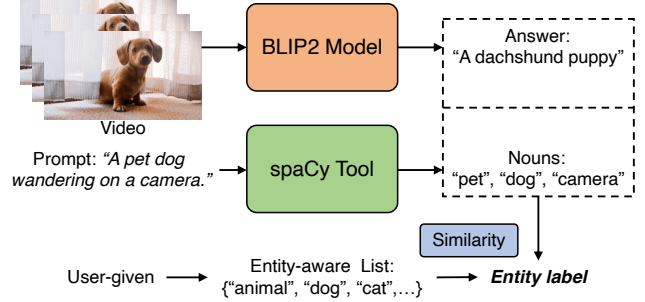


Figure 4. The overview of the data process. To enhance the entity segmentation accuracy, we employ the BLIP2 model. We also construct a user-given entity-aware list to generate data for a specific entity category. The entity label is calculated with similarity.

the requisite training set, shown in Fig. 4. However, the labeled captions of videos are not precise enough, especially to get the label of entity segmentation. To address this issue, we utilize BLIP-2 [20] to generate more precise captions. Specifically, given a video containing  $m$  frames  $\mathcal{V} = \{v_i | i \in [1, m]\}$  with its original caption  $\mathcal{P}$ , we select the first frame  $v_1$  and use BLIP-2 to get more information. We set the question “*What is the foreground in the picture?*” for BLIP-2 and get the answer  $\mathcal{A}$ . At the same time, the origin prompt  $\mathcal{P}$  is handled with spaCy tool to extract nouns  $\mathcal{S} = \{s_i | i \in [1, n]\}$ . To ensure the accuracy of entity labels, we maintain a user-given entity-aware list  $\mathcal{W}$  to prioritize entities for a certain topic, which contains words of some specific domains, such as “*animal, dog, cat, ...*”.

---

#### Algorithm 1: Entity label selection.

---

**Input:**  $\mathcal{A}, \mathcal{W}, \mathcal{S} = \{s_i | i \in [1, n]\}$ .

**Output:**  $e$ : entity label.

```

1 scores1 = List(), scores2 = List()
2 for i = 0 to length(W) do
3   scores1.append(Similarity(A, Wi))
4   for j = 0 to length(S) do
5     scores2.append(Similarity(Sj, Wi))
6 if max(scores1) > θ then e = A;
7 else e = max(scores2);

```

---

We calculate the distance metric to quantify the disparity between the answer  $\mathcal{A}$  and each word within the list  $\mathcal{W}$ . Subsequently, we assess the similarity between the words in  $\mathcal{W}$  and each noun in the entity-aware list  $\mathcal{S}$ , individually. The selection process is defined in Algorithm 1. Once we get the entity label, we use SAM-Track [7] to capture the entity mask of each frame. Furthermore, we append the final entity label to the original video caption, thereby generating an augmented caption. In the last step, we merge the video-text pairs with segmentation masks for model training.

## 4. Experiments

### 4.1. Experimental Setups

**Data for Training.** Considering the quality of the video content, we select the Pexel Videos dataset<sup>1</sup> to serve as the training data. The dataset contains abundant videos with high quality, each averaging 19.5 seconds in duration. Owing to the lack of entity labels within the original data, we apply the processing approach detailed in Sec. 3.4 to enhance the dataset’s utility for our purposes. We process 76,303 videos for training and 100 videos for evaluation. In addition, we use the pre-trained model of VidRD [9], which is trained on 5.3M video data.

**Evaluation Metrics.** We evaluate our proposed VideoAssembler using two aspects of metrics:

(i) Metrics for video quality evaluation. Previous works like [1, 8, 37] use two metrics for quantitative evaluation, i.e., **Fréchet Video Distance (FVD)** [40] and **Video Inception Score (IS)** [35]. FVD is a video quality evaluation metric based on FID [28]. Following [37], we use a trained I3D model [3] for calculating FVD. Following previous works [1, 13, 37], a trained C3D model [39] is used for calculating the video version of IS.

(ii) Metrics for identity consistency and video-prompt alignment. a) We compute the **DINO score** [34] between the generated entity and the given entity to evaluate the entity fidelity. b) Following [44], we calculate the average cosine similarity between all pairs of video frames to evaluate the **Frame-consistency**. We calculate the average CLIP score between all frames of generated videos and corresponding prompts to evaluate the **Textual-alignment**.

### 4.2. Main Results

There is no existing work for identity-consistent video generation with reference entities to directly compare with. However, our framework is flexible and allows us to control the number of reference entities for different tasks, such as image-to-video generation with single or multiple frames or video editing with a video. Furthermore, the generative aspect of our VideoAssembler is regulated through textual prompts, thus our comparative analysis primarily encompasses the domains of text-to-video, image-to-video synthesis, and video editing tasks.

**Quantitative Evaluation.** To prove the efficiency of the proposed VideoAssembler, we conduct the generative performance on UCF-101 [38], which has 101 brief class names (10,000 videos for test). The dataset which is commonly employed to assess the generation performance of various methods, such as works [13, 37, 42]. To acquire the necessary reference entity images for our method, we preprocess the UCF-101 video dataset employing the same

<sup>1</sup><https://huggingface.co/datasets/Corran/pixelvideos>

Model	Videos for Training	IS ↑	FVD ↓
CogVideo [13]	5.4M	25.27	701.59
MagicVideo [49]	27.0M	-	699.00
LVDM [10]	2.0M	-	641.80
Video LDM [1]	10.7M	33.45	550.61
Make-A-Video [37]	20.0M	33.00	367.23
VideoFactory [42]	140.7M	-	410.00
PYoCo [8]	22.5M	47.76	355.19
I2VGen-XL [48]	10.3M	18.90	597.49
<b>VideoAssembler</b>	<b>5.3M+76K</b>	<b>48.01</b>	<b>346.84</b>

Table 1. Quantitative evaluation results on UCF-101. The second and third rows show text-to-video and image-to-video (in gray) methods. All the videos for evaluation are generated in a zero-shot manner. In comparison with other methods, VideoAssembler achieves the best metrics while using fewer videos for training.

steps as delineated for our training data preparation. For inference on the UCF-101 dataset, we utilize a singular textual prompt and four reference entities. Tab. 1 shows the FVD and IS results. It is discernible that our method exhibits good performance when benchmarked against other SOTA approaches. The outcomes further indicate that our method is capable of generating videos with superior performance metrics. Noticed that most of the existing image-to-video methods do not report quantitative results, but only provide visualized examples, such as [5, 25].

Model	Videos for Training	IS ↑	FVD ↓
CogVideo [13]	5.4M	-	1294
MagicVideo [49]	27.0M	-	998
I2VGen-XL [48]	10.3M	10.52	341.72
<b>VideoAssembler</b>	<b>5.3M+76K</b>	<b>15.79</b>	<b>252.0</b>

Table 2. Results on MSR-VTT. The second and third rows show text-to-video and image-to-video methods (in gray), respectively.

We also conduct a zero-shot comparison with methods [13, 48, 49] on the MSR-VTT dataset (2,990 videos). The results of FVD and IS metrics are reported in Tab. 2, which show that our proposed method surpasses its counterparts in performance metrics. Noticed that our method is 89.72 higher than I2VGen-XL, which is an image-to-video generation work, on the FVD metric. Besides, to demonstrate the fidelity and identity consistency of entities within the videos synthesized by VideoAssembler, we employ the DINO score, Textual-align, and Frame-consistency for evaluative purposes on the UCF-101 and MSR-VTT compared with [48]. The results are shown in Tab. 3, which indicate that the videos we generate have good text alignments, and

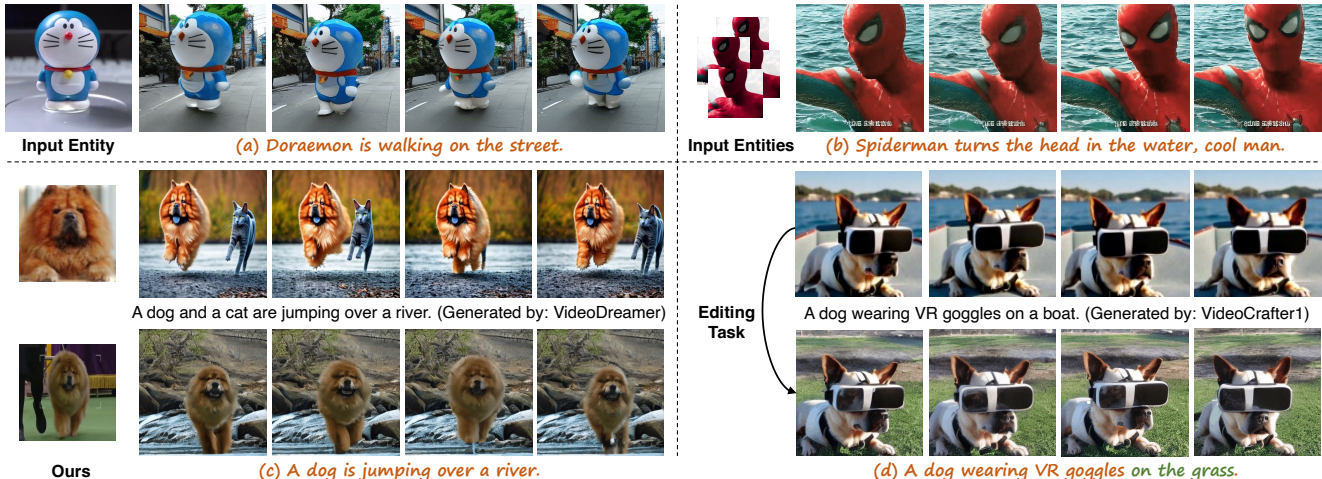


Figure 5. Qualitative results and comparison between our VideoAssembler and VideoDreamer [4], which also is an entity driven method. Our method demonstrates superior entity fidelity and action control compared to it, as evidenced by (example c). Moreover, our model exhibits finer motion control (examples a, b) and good performance in video editing (example d).

the continuity between frames is also commendable.

Methods	DINO	Textual-align	Frame-consist
I2VGen-XL [48]	44.1	21.34	89.40
<b>VideoAssembler</b>	<b>50.8</b>	<b>25.41</b>	<b>90.22</b>
I2VGen-XL [48]	42.7	18.42	<b>89.77</b>
<b>VideoAssembler</b>	<b>49.5</b>	<b>21.57</b>	84.76

Table 3. Results of DINO, textual-alignment, and frame-consistency on UCF-101 and MSR-VTT. The white part is the result of UCF-101, and the gray part is the result of MSR-VTT.

**Human Evaluations.** We perform human evaluations of our method, which is conducted by a panel of 34 human raters, over 15 videos with corresponding prompts. We adopt the Likert Scale [22] to evaluate entity fidelity, prompt alignment, and the quality of the generated videos. The range of these three scores is between 1 and 5, which represents from very dissatisfied to very satisfied. We show the results of human evaluations in Tab. 4. Because there is no similar work that can be directly compared, we tend to focus more on user satisfaction for the videos we generate when designing user evaluations. Our method achieves high scores on both entity fidelity and text alignment, as well as producing high-quality videos. These results indicate that our method performs well under human evaluation and demonstrates its superiority over existing methods.

**Performance of Video Editing.** In addition, we put the whole video into VideoAssembler to achieve video editing. we evaluate the CLIP-Score of text and image on the DAVIS, which is built by [14] for video editing test. The results compared with [2, 30] are shown in Tab. 5.

Scores	VideoAssembler
<b>Entity Fidelity</b>	4.16
<b>Prompt Alignment</b>	4.09
<b>Quality</b>	3.72

Table 4. Results of human evaluations. The value indicates the degree of user satisfaction with the generated content, which is an absolute measure with a maximum score of 5 at the design stage.

Methods	Textual-align	Frame-consistency
Framewise IP2P [2]	25.11	86.76
FateZero [30]	23.81	<b>92.92</b>
<b>VideoAssembler</b>	<b>27.65</b>	89.43

Table 5. Results of video editing on DAVIS dataset. Noticed that method [2] can only perform image editing, and for comparison, we repeated the evaluation of its generated video frames.

**Qualitative Evaluation.** We show the qualitative results and comparisons with VideoDreamer [4] in Fig. 5. We delineate four distinct configurations for analysis: input with a single entity, input with multiple entities, utilization of the same entity as in VideoDreamer, and the video editing task. In the context of video editing, we utilize content originally synthesized by VideoCrafter1 [5] as our foundational material. When contrasted with VideoDreamer, as illustrated in example (c), the superior fidelity with which our method renders the input entity is apparent. Examples (a) and (b) demonstrate our model’s adaptability to either single or multiple entity inputs, while example (d) showcases its proficient editing capabilities.

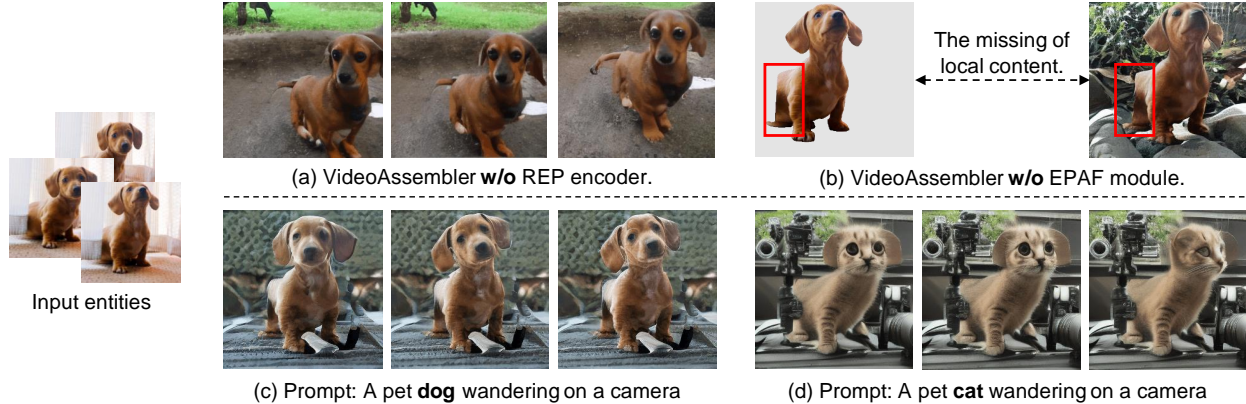


Figure 6. We present the outcomes of VideoAssembler without the REP and EPAF in examples (a, b), respectively. Selection of the entity as a dog, accompanied by subsequent text replacement with 'dog' and 'cat' in examples (c, d), and show the model’s control ability.

### 4.3. Ablation Studies

Frames	IS $\uparrow$	FVD $\downarrow$
$n = 1$	47.02	406.69
$n = 4$	48.01	<b>346.84</b>
$n = 8$	<b>49.13</b>	506.61
$n = 1$	17.40	283.14
$n = 4$	15.79	<b>252.05</b>
$n = 8$	<b>19.10</b>	324.17

Table 6. Effect of the quantity of the input entity. The white part is the result of UCF-101, and the gray part is the result of MSR-VTT.

**Effects of Input Entity Quantity.** Given that our method accommodates a diverse array of inputs encompassing varying numbers of entities, we devise an experiment to ascertain the impact of varying the number of input frames, denoted as  $n$ . Our evaluation strategy involves assessing the algorithm with distinct input configurations: singular (1) and multiple (4 and 8). We use FVD and IS on UCF-101 and IS on MSR-VTT to evaluate our method. Analysis of the data in Tab. 6 reveals that the IS metric achieves optimal performance at  $n = 8$ , while the FVD metric records its best performance at  $n = 4$ . Due to the minimal fluctuation of the IS index under different  $n$  values, we consider the model to perform best when  $n = 4$ . This also suggests that our approach requires only a minimal number of entities to accomplish high-quality video generation.

**Effects of the REP Encoder and the EPAF Module.** Within our VideoAssembler framework, the REP encoder principally assimilates detailed appearance to enhance the fidelity of input entities. Concurrently, the EPAF module integrates text-alignment attributes of the entities into the denoising process, enriching the model’s capability. To assess each part’s effectiveness, we evaluate the model separately without the REP encoder and EPAF module. We show the

visualization results in Fig. 6. Examples (a) and (b) demonstrate that the inclusion of our REP encoder is crucial for maintaining the fidelity of the input entities. This substantiates that the features introduced into the cross-attention layer are predominantly semantic in nature, akin to the approach employed by Method [43]. Moreover, it can be observed that the exclusive use of the REP encoder may impinge upon the generative creativity of the model, thereby diminishing its text-alignment capability. Case (b) illustrates this phenomenon, indicating that in instances where foreground content is lacking, the REP encoder fails to reconcile the generated content with its semantic counterpart.

**Effects of Prompts for Identical Entities.** To discern the dominant influence between textual prompts and input entities, given their dual control mechanism, we design an experiment as follows: for a given entity image, we input text descriptions that are either congruent or incongruent with the entity’s category. When given an entity image of a dog, we assess the prompts “dog” and “cat”. The corresponding results are illustrated in examples (c, d) of Fig. 6. The analysis reveals that while the prompt exerts control over the generated video, the overarching structure of the content is also steered by the entity. This affirms that our method can blend the entity in the video and control it with prompts.

## 5. Conclusion

In this work, we proposed a novel end-to-end method for video generation with reference entities, named VideoAssembler. It can conduct direct inference when giving new entities. The REP and EPAF modules guarantee adaptable control over both entity and prompt. Moreover, our model can handle inputs with varying numbers of entities, which makes it a flexible framework for both generation and editing tasks. We conducted extensive experiments to demonstrate that our method achieves high performance in both quantitative and qualitative evaluations.



## References

- [1] Andreas Blattmann, Robin Rombach, Huan Ling, Tim Dockhorn, Seung Wook Kim and Sanja Fidler, and Karsten Kreis. Align your latents: High-resolution video synthesis with latent diffusion models. In *CVPR*, pages 22563–22575, 2023. 2, 6
- [2] Tim Brooks, Aleksander Holynski, and Alexei A. Efros. Instructpix2pix: Learning to follow image editing instructions. In *CVPR*, pages 18392–18402, 2023. 7
- [3] Joao Carreira and Andrew Zisserman. Quo vadis, action recognition? a new model and the kinetics dataset. In *CVPR*, pages 6299–6308, 2017. 6
- [4] Hong Chen, Xin Wang, Guanning Zeng, Yipeng Zhang, Yuwei Zhou, Feilin Han, and Wenwu Zhu. Videodreamer: Customized multi-subject text-to-video generation with disen-mix finetuning. *arXiv preprint arXiv:2311.00990*, 2023. 2, 3, 7
- [5] Haoxin Chen, Menghan Xia, Yingqing He, Yong Zhang, Xiaodong Cun, Shaoshu Yang, Jinbo Xing, Yaofang Liu, Qifeng Chen, Xintao Wang, Chao Weng, and Ying Shan. Videocrafter1: Open diffusion models for high-quality video generation. *arXiv preprint arXiv:2310.19512*, 2023. 2, 3, 4, 5, 6, 7
- [6] Tsai-Shien Chen, Chieh Hubert Lin, Hung-Yu Tseng, Tsung-Yi Lin, and Ming-Hsuan Yang. Motion-conditioned diffusion model for controllable video synthesis. *arXiv preprint arXiv:2304.14404*, 2023. 3
- [7] Yangming Cheng, Liulei Li, Yuanyou Xu, Xiaodi Li, Zongxin Yang, Wenguan Wang, and Yi Yang. Segment and track anything. *arXiv preprint arXiv:2305.06558*, 2023. 5
- [8] Songwei Ge, Seungjun Nah, Guilin Liu, Tyler Poon, Andrew Tao, Bryan Catanzaro, David Jacobs, Jia-Bin Huang, Ming-Yu Liu, and Yogesh Balaji. Preserve your own correlation: A noise prior for video diffusion models. In *CVPR*, pages 22930–22941, 2023. 2, 4, 6
- [9] Jiayi Gu, Shicong Wang, Haoyu Zhao, Tianyi Lu, Xing Zhang, Zuxuan Wu, Songcen Xu, Wei Zhang, Yu-Gang Jiang, and Hang Xu. Reuse and diffuse: Iterative denoising for text-to-video generation. *arXiv preprint arXiv:2309.03549*, 2023. 2, 3, 6
- [10] Yingqing He, Tianyu Yang, Yong Zhang, Ying Shan, and Qifeng Chen. Latent video diffusion models for high-fidelity video generation with arbitrary lengths. *arXiv preprint arXiv:2211.13221*, 2022. 6
- [11] Jonathan Ho, William Chan, Chitwan Saharia, Jay Whang, Ruiqi Gao, Alexey Gritsenko, Diederik P. Kingma, Ben Poole, Mohammad Norouzi, David J. Fleet, and Tim Salimans. Imagen video: High definition video generation with diffusion models. *arXiv preprint arXiv:2210.02303*, 2022. 2, 4
- [12] Jonathan Ho, Tim Salimans, Alexey Gritsenko, William Chan, Mohammad Norouzi, and David J. Fleet. Video diffusion models. *arXiv preprint arXiv:2204.03458*, 2022. 2
- [13] Wenyi Hong, Ming Ding, Wendi Zheng, Xinghan Liu, and Jie Tang. Cogvideo: Large-scale pretraining for text-to-video generation via transformers. In *ICLR*, 2023. 2, 6
- [14] Wu Jay Zhangjie, Gao Difei, Bai Jinbin, Shou Mike, Li Xiyu, Dong Zhen, Singh Aishani, Keutzer Kurt, and Landola Forrest. Loveu@cvpr’23 - track4, 2023. 2, 7
- [15] Yujin Jeong, Wonjeong Ryoo, Seunghyun Lee, Dabin Seo, Wonmin Byeon, Sangpil Kim, and Jinkyu Kim. The power of sound (tpos): Audio reactive video generation with stable diffusion. In *ICCV*, 2023. 3
- [16] Ho Jonathan and Salimans Tim. Classifier-free diffusion guidance. *arXiv preprint arXiv:2207.12598*, 2022. 2
- [17] Ho Jonathan, Jain Ajay, and Abbeel Pieter. Denoising diffusion probabilistic models. *Advances in Neural Information Processing Systems*, 33:6840–6851, 2020. 2
- [18] Johanna Karras, Aleksander Holynski, Ting-Chun Wang, and Ira Kemelmacher-Shlizerman. Dreampose: Fashion image-to-video synthesis via stable diffusion. *arXiv preprint arXiv:2304.06025*, 2023. 2, 3
- [19] Preechakul Konpat, Chatthee Nattanat, Wizadwongsa Suttisak, and Suwajanakorn Supasorn. Diffusion autoencoders: Toward a meaningful and decodable representation. In *CVPR*, pages 10619–10629, 2022. 2
- [20] Junnan Li, Dongxu Li, Silvio Savarese, and Steven Hoi. Blip-2: Bootstrapping language-image pre-training with frozen image encoders and large language models. *arXiv preprint arXiv:2301.12597*, 2023. 5
- [21] Zhengqi Li, Richard Tucker, Noah Snaveley, and Aleksander Holynski. Generative image dynamics. *arXiv preprint arXiv:2309.07906*, 2023. 3
- [22] Rensis Likert. A technique for the measurement of attitudes. *Archives of psychology*, 1932. 7
- [23] Jian Ma, Junhao Liang, Chen Chen, and Haonan Lu. Subject-diffusion: Open domain personalized text-to-image generation without test-time fine-tuning. *arXiv preprint arXiv:2307.11410*, 2023. 2, 3, 4, 5
- [24] Yue Ma, Yingqing He, Xiaodong Cun, Xintao Wang, Ying Shan, Xiu Li, and Qifeng Chen. Follow your pose: Pose-guided text-to-video generation using pose-free videos. *arXiv preprint arXiv:2304.01186*, 2023. 3
- [25] Eyal Molad, Eliahu Horwitz, Dani Valevski, Alex Rav Acha, Yossi Matias, Yael Pritch, Yaniv Leviathan, and Yedid Hoshen. Dreamix: Video diffusion models are general video editors. *arXiv preprint arXiv:2302.01329*, 2023. 2, 3, 4, 6
- [26] Liu Nan, Li Shuang, Du Yilun, Torralba Antonio, and Joshua B Tenenbaum. Compositional visual generation with composable diffusion models. In *ECCV*, pages 423–439, 2022. 2
- [27] Haomiao Ni, Changhao Shi, Kai Li, Sharon X. Huang, and Martin Renqiang Min. Conditional image-to-video generation with latent flow diffusion models. In *CVPR*, pages 18444–18455, 2023. 2, 3
- [28] Gaurav Parmar, Richard Zhang, and Jun-Yan Zhu. On aliased resizing and surprising subtleties in gan evaluation. In *CVPR*, pages 11410–11420, 2022. 6
- [29] Dhariwal Prfulla and Nichol Alexander. Diffusion models beat gans on image synthesis. *Advances in Neural Information Processing Systems*, 34:8780–8794, 2021. 2
- [30] Chenyang Qi, Xiaodong Cun, Yong Zhang, Chenyang Lei, Xintao Wang, Ying Shan, and Qifeng Chen. Fatezero: Fus-

- ing attentions for zero-shot text-based video editing. *arXiv preprint arXiv:2303.09535*, 2023. 7
- [31] Bosheng Qin, Wentao Ye, Qifan Yu, Siliang Tang, and Yuet-ing Zhuang. Dancing avatar: pose and text-guided human motion videos synthesis with image diffusion model. *arXiv preprint arXiv:2308.07749*, 2023. 3
- [32] Nichol Alexander Quinn and Dhariwal Prafulla. Improved denoising diffusion probabilistic models. *arXiv preprint arXiv:2102.09672*, 2021. 2
- [33] Robin Rombach, Andreas Blattmann, Dominik Lorenz, Patrick Esser, and Björn Ommer. High-resolution image synthesis with latent diffusion models. In *CVPR*, pages 10684–10695, 2022. 2, 5
- [34] Nataniel Ruiz, Yuanzhen Li, Varun Jampani, Yael Pritch, Michael Rubinstein, and Kfir Aberman. Dreambooth: Fine tuning text-to-image diffusion models for subject-driven generation. In *CVPR*, pages 22500–22510, 2023. 3, 6
- [35] Masaki Saito, Shunta Saito, Masanori Koyama, and Sosuke Kobayashi. Generate densely: Memory-efficient unsupervised training of high-resolution temporal gan. *IJCV*, 128: 2586–2606, 2020. 6
- [36] Christoph Schuhmann, Romain Beaumont, Richard Vencu, Cade Gordon, Ross Wightman, Mehdi Cherti, Theo Coombes, Aarush Katta, Clayton Mullis, Mitchell Wortsman, Patrick Schramowski, Srivatsa Kundurthy, Katherine Crowson, Ludwig Schmidt, Robert Kaczmarczyk, and Jenia Jitsev. Laion-5b: An open large-scale dataset for training next generation image-text models. *Advances in Neural Information Processing Systems*, 35:25278–25294, 2022. 5
- [37] Uriel Singer, Adam Polyak, Thomas Hayes, Xi Yin, Jie An, Songyang Zhang, Qiyuan Hu, Harry Yang, Oron Ashual, Oran Gafni, Devi Parikh, Sonal Gupta, and Yaniv Taigman. Make-a-video: Text-to-video generation without text-video data. *arXiv preprint arXiv:2209.14792*, 2022. 2, 6
- [38] Khurram Soomro, Amir Roshan Zamir, and Mubarak Shah. Ucf101: A dataset of 101 human actions classes from videos in the wild. *arXiv preprint arXiv:1212.0402*, 2012. 2, 6
- [39] Du Tran, Lubomir Bourdev, Rob Fergus, Lorenzo Torresani, and Manohar Paluri. Learning spatiotemporal features with 3d convolutional networks. In *ICCV*, pages 4489–4497, 2015. 6
- [40] Thomas Unterthiner, Sjoerd van Steenkiste, Karol Kurach, Raphael Marinier, Marcin Michalski, and Sylvain Gelly. Fvd: A new metric for video generation. *ICLR Workshop*, 2019. 6
- [41] Tan Wang, Linjie Li, Kevin Lin, Yuanhao Zhai, Chung-Ching Lin, Zhengyuan Yang, Hanwang Zhang, Zicheng Liu, and Lijuan Wang. Disco: Disentangled control for realistic human dance generation. *arXiv preprint arXiv:2307.00040*, 2023. 3
- [42] Wenjing Wang, Huan Yang, Zixi Tuo, Huiguo He, Junchen Zhu, Jianlong Fu, and Jiaying Liu. Videofactory: Swap attention in spatiotemporal diffusions for text-to-video generation. *arXiv preprint arXiv:2305.10874*, 2023. 2, 6
- [43] Xiang Wang, Hangjie Yuan, Shiwei Zhang, Dayou Chen, Jiuniu Wang, Yingya Zhang, Yujun Shen, Deli Zhao, and Jingren Zhou. Videocomposer: Compositional video synthesis with motion controllability. *arXiv preprint arXiv:2306.02018*, 2023. 2, 3, 4, 5, 8
- [44] Jay Zhangjie Wu, Yixiao Ge, Xintao Wang, Weixian Lei, Yuchao Gu, Yufei Shi, Wynne Hsu, Ying Shan, Xiaohu Qie, and Mike Zheng Shou. Tune-a-video: One-shot tuning of image diffusion models for text-to-video generation. In *ICCV*, pages 7623–7633, 2023. 6
- [45] Jun Xu, Tao Mei, Ting Yao, and Yong Rui. Msr-vtt: A large video description dataset for bridging video and language. In *CVPR*, pages 5288–5296, 2016. 2
- [46] Shengming Yin, Chenfei Wu, Jian Liang, Jie Shi, Houqiang Li, Gong Ming, and Nan Duan. Dragnuwa: Fine-grained control in video generation by integrating text, image, and trajectory. *arXiv preprint arXiv:2308.08089*, 2023. 3
- [47] Lvmin Zhang, Anyi Rao, and Maneesh Agrawala. Adding conditional control to text-to-image diffusion models. In *CVPR*, pages 3836–3847, 2023. 2
- [48] Shiwei Zhang, Jiayu Wang, Yingya Zhang, Kang Zhao, Hangjie Yuan, Zhiwu Qin, Xiang Wang, Deli Zhao, and Jingren Zhou. I2vgen-xl: High-quality image-to-video synthesis via cascaded diffusion models. *arXiv preprint arXiv:2311.04145*, 2023. 3, 6, 7
- [49] Daquan Zhou, Weimin Wang, Hanshu Yan, Weiwei Lv, Yizhe Zhu, and Jiashi Feng. Magicvideo: Efficient video generation with latent diffusion models. *arXiv preprint arXiv:2211.11018*, 2022. 6